SINTERING CHARACTERISTICS AND CHARACTERISATION OF Al-Mn-Ce NANOSTRUCTURED MATERIAL PREPARED BY MECHANICAL ALLOYING

A THESIS SUBMITTED IN PARTIAL FULFILLMENT OF THE REQUIREMENTS FOR THE DEGREE OF

Bachelor of Technology In

Metallurgical and Materials Engineering

By

DEEPANJAN ROY (Roll NO. 10404017)

SHANTANU RAI (Roll No. 10404021)

UNDER THE GUIDANCE OF

PROF. S. MULA

PROF (Mrs). A. MALLIK

Department of Metallurgical and Materials Engineering

National Institute of Technology

Rourkela

National Institute of Technology
Rourkela

CERTIFICATE

This is to certify that the thesis entitled, “Sintering Characteristics And Characterisation Of Al-Mn-Ce Nanostructured Material Prepared By Mechanical Alloying” submitted by Deepanjan Roy and Shantanu Rai in partial fulfillment of the requirements for the award of Bachelor of Technology Degree in Metallurgical and Materials Engineering at the National Institute of Technology, Rourkela is an authentic work carried out by them under our supervision and guidance .To the best of our knowledge, the matter embodied in the thesis has not been submitted to any other University / Institute for the award of any Degree or Diploma.

Date:

Prof. S. Mula

Prof.(Mrs) A. Mallik

ACKNOWLEDGEMENT

During the entire project work, we have received endless help and guidance from Prof. A. Mallik and Prof. S. Mula right from deciding the topic till the final presentations. We wish to express our deep gratitude to all those who extended their helping hands towards us in various ways during our one year project work. We really appreciate the support we have received during our project from our guides who were available not only within institute hours but beyond that .We are thankful to Prof.S.Mula and Prof. A. Mallik who gave us all the facilities and resources at their disposal that were needed for our project work. We would like to express our sincere thanks to the department of Metallurgical and Materials Engineering for allowing us to access the computers in the lab for hours together. We are also thankful to Mr. Uday Kr. Sahu, Mr. S. Hembrahm, Mr. Rajesh Patnaik and Mr. Samir for their help in the experimental procedures.

Date:

Deepanjan Roy Shantanu Rai

Dept. of Metallurgical and Materials Engineering

National Institute of Technology

Rourkela -769008

CONTENTS

Page No.

List of figures:

ABSTRACT

Nanomaterials are experiencing a rapid development in recent years due to their existing and/or potential applications in a wide variety of technological areas such as electronics, catalysis, ceramics, magnetic data storage, structural components etc. To meet the technological demands in these areas, the size of the materials should be reduced to the nanometer scale. As the size reduces into the nanometer range, the materials exhibit peculiar and interesting mechanical and physical properties, e.g. increased mechanical strength, enhanced diffusivity, higher specific heat and electrical resistivity compared to conventional coarse grained counterparts. There are various routes of synthesis of nanocomposites which have been discussed at length later in this paper and out of all of these we have opted for mechanical alloying as the route for synthesizing Al-Mn-Ce nanocomposite.

Powder blends of elemental (>99.5 wt % purity) Al, Mn and Ce (<70 μm particle size) having nominal compositions of $Al_{90}Mn_8Ce_2$ (in at. %) were ball milled in a planetary mill. Ball to powder ratio was maintained at 10:1 throughout milling operation. The powder sample we have deployed various characterization techniques viz. XRD, SEM, EDS, and FTIR to study the properties of the nanocomposites. Final powder milled for 86 h was compacted at loads of 10-12 tonnes. These specimens were measured for green density and subsequently sintered in nitrogen and hydrogen atmospheres at different temperatures. After sintering, sintered compacts were again analyzed for density and X-ray diffraction.

XRD of powder material shows a compound formation between Al, Mn and Ce .The particles have become finer as a function of milling time as revealed by broadening of the XRD peaks. XRD calculations based on Scherrer formula indicate decreasing crystallite size and increasing lattice strain with increasing milling h. SEM micrographs show distinct Al rich and alloy rich region. Critical analysis of these regions has been done using EDS. FTIR results indicate increasing % absorbance and decreasing % transmittance as crystallite size decreases. We observe that specimens sintered at 600°C in N_2 and H_2 atmospheres have high hardness values of 147VHN and 148VHN respectively. This can be attributed to the high green density values of around 68% which after sintering attained a value of around 75%.Another reason for the high hardness is the presence of hard AlN and AlH_3 phases. Specimens sintered at 650 and 675°C, although expected to exhibit higher hardness values have been found to have much lower hardness values of 50 and 51VHN

respectively. This anomaly can be attributed to the lower green density (approx. 57%) of the specimens which after sintering attained a density of around 65% only.

CHAPTER 1

INTRODUCTION

Nanomaterials are experiencing a rapid development in recent years due to their existing and/or potential applications in a wide variety of technological areas such as electronics, catalysis, ceramics, magnetic data storage, structural components etc. To meet the technological demands in these areas the size of the materials should be reduced to the nanometer scale. For example, the miniaturization of functional electronic devices demands the placement or assembly of nanometer scale components into well-defined structures. As the size reduces into the nanometer range, the materials exhibit peculiar and interesting mechanical and physical properties, e.g. increased mechanical strength, enhanced diffusivity, higher specific heat and electrical resistivity compared to conventional coarse grained counterparts [1]. It has been stimulated by the interest for basic scientific investigations and their technological applications. Nanomaterials and most of the applications derived from them are still in an early stage of technical development. There are several issues that remain to be addressed before nanomaterial will become potentially useful for industrial sectors. These issues include synthesis of high purity materials with large yield economically and environmentally, characterization of new structures and properties of nanophase materials ,fabrication of dense products from nano particles with full density and less contamination, and retention of the ultrafine grain size in service in order to preserve the mechanical properties associated with the nanometer scale [2].

The aerospace industry is continuously pursuing to enhance the performance of commercial and military aircraft and thus, driving the development of better high performance structural materials. In recent years, metal matrix composites (MMC) have emerged as a promising class of such materials. MMCs often have a relatively ductile metal matrix phase and a significantly harder reinforcement material like ceramics or refractory metals. The matrix holds the reinforcement material together and provides ductility.

The reinforcement imparts strength and stiffness to the composite [3]. A common problem with MMCs is the difficulty creating a strong matrix/reinforcement interface without suffering extensive dissolution, de-bonding [3], or chemical reactions. A proposed solution is the use of a reinforcement material which is similar in chemistry to the matrix. Many studies have been dedicated to aluminum and its alloys as matrix due to their lightweight cost, and their unique thermal properties that have enormous space and avionics prospects.

Materials reduced to the nanoscale can suddenly show very different properties compared to what they exhibit on a macro scale, enabling unique applications. For instance, opaque substances become transparent (copper); inert materials become catalysts (platinum); stable materials turn combustible (aluminum); solids turn into liquids at room temperature (gold); insulators become conductors (silicon). Materials such as gold, which is chemically inert at normal scales, can serve as a potent chemical catalyst at nanoscales [4]. Much of the fascination with nanotechnology stems from these unique quantum and surface phenomena that matter exhibits at the nanoscale.

Nanosize powder particles (a few nanometers in diameter, also called nano-particles are potentially important in ceramics, powder metallurgy, the achievement of uniform nano porosity and similar applications. The strong tendency of small particles to form clumps ("agglomerates") is a serious technological problem that impedes such applications. However, a few dispersants such as ammonium citrate (aqueous) and imidazoline or oleyl alcohol (non aqueous) are promising additives for de-agglomeration [4].

CHAPTER 2

LITERATURE SURVEY

2.1Metal matrix composites (MMC)

Metal matrix composites cover a relatively wide range of materials defined by the metal matrix, reinforcement geometry and type. In the matrix field, most metallic systems have been studied and explored. They include aluminum, beryllium, magnesium, titanium, iron, nickel, cobalt, and silver but aluminum is by far the preferred one [5]. MMCs consist of at least two constituent parts, the major percentage of one being a metal and the other part may be a different metal or another material, such as a ceramic or organic compound. When at least three materials are present, it is called hybrid composite. An MMC is complementary to a cermet. These engineering materials can attain higher strength, greater stiffness, and better dimensional stability than the unreinforced metal alloys which promoted the development of varied kinds of MMC of low cost, lighter and stronger than their original alloys [5,3]. Incorporating the two materials (the matrix and the reinforcement materials) result in remarkable structural and physical properties.

In a metal matrix composite the two constitutive parts are:

The matrix, which is the monolithic material where the reinforcement is embedded, and is fully continuous. Furthermore there is a pathway through the matrix to any point in the material where dissimilar two materials sandwiched together. The matrix is usually a lighter metal such as aluminum, magnesium, or titanium, and provides a compliant support for the reinforcement to be used in structural applications [3]. The reinforcement is embedded into the matrix and can be divided into five major categories: continuous fibers, discontinuous fibers, whiskers, particulates, and wires. Reinforcements generally are

ceramics with the exception of wires, which are metals. They can be either continuous, or discontinuous.

1. Discontinuous MMCs can be isotropic and worked with standard metalworking techniques. These use whiskers, short fibers, or particles. The most common reinforcing materials in this category are alumina and silicon carbide [3].

2. Continuous reinforcement uses monofilament wires or fibers such as carbon fiber or silicon carbide. Because the fibers are embedded into the matrix in a certain direction, the result is an anisotropic structure in which the alignment of the material affects its strength. Some of the first MMCs used boron fibers as reinforcement [3]. The wide diversity of MMCs has properties that differ dramatically. The factors influencing their characteristics include: matrix and reinforcement properties, form, geometric arrangement, volume fraction, including effects of porosity and the interface between the matrix and reinforcement.

Aluminum matrix composites (AMC)

AMCs are the most important and attractive non-ferrous matrix materials used particularly in the aerospace and transport industry where light weight of structural components is crucial. Aluminum composites have unique thermal and conductive properties with coefficient of expansion that can be tailored down to zero. Parameters like the matrix alloy and reinforcement material, and volume, shape and location of the reinforcement, as well as the fabrication method can all be varied to achieve required properties [3]. Regardless of the variations, however, aluminium composites offer the advantage of low cost over most other MMCs. In addition, they offer high shear strength, excellent abrasion resistance, high-temperature operation, non-flammability, minimal attack by fuels and solvents, and the ability to be formed and treated on conventional equipment. They are very attractive for

their isotropic mechanical properties (higher than their unreinforced alloys) and their low costs, cheap processing routes and low prices of some of the discontinuous reinforcement such as SiC particles or Al_2O_3 short fibers.

2.2Properties of Nanomaterials

Nano-structured materials are a broad class of materials, with microstructures modulated in zero to three dimensions on length scales less than 100 nm. These materials are atoms arranged in nanosized clusters, which become the constituent grains or building blocks of the material. Conventional materials have grains sizes ranging from microns to several millimeters and contain several billion atoms each. Nanometer sized grains contain only about 900 atoms each [2]. As the grain size decreases, there is a significant increase in the volume fraction of grain boundaries or interfaces. This characteristic strongly influences the chemical and physical properties of the material. Nanophase metals exhibit significant increases in yield strength and elastic modulus. It has also been shown that other considerable interest in the generation of carbon nanostructures, which are related to the famous Bucky ball. In addition, the use of nano-sized materials as fillers for composite materials is generating interest .Specifically in the case of polymer nanocomposites [2,6]. All materials are composed of grains, which in turn comprise many atoms. These grains are usually invisible to the naked eye, depending on their size. Conventional materials have grains varying in size anywhere from 100's of microns (μm) to millimeters (mm). A nanometer (nm) is even smaller a dimension than a μm, and is a billionth (10^{-9}) of a meter. A nano crystalline material has grains on the order of 1-100 nm. The average size of an atom is on the order of 1 to 2 angstroms (Å) in radius. 1 nanometer comprises 10 Å, and hence in one nm, there may be 3-5 atoms, depending on the atomic radii. Nanocrystalline materials are exceptionally strong, hard, and ductile at high temperatures, wear-resistant, erosion resistant, corrosion-resistant, and chemically very active. Nano-crystalline materials, or nano-materials, are also much more formable than their conventional, commercially available counterparts [6].

2.3 Advantages of Nanosized Additions

The Nano-composites 2000 conference [4] has revealed clearly the property advantages that nano-material additives can provide in comparison to both their conventional filler counterparts and base polymer. Properties which have been shown to undergo substantial improvements include:

· Mechanical properties e.g. strength, modulus and dimensional stability

· Decreased permeability to gases, water and hydrocarbons

· Thermal stability and heat distortion temperature

· Flame retardancy and reduced smoke emissions

· Chemical resistance

· Surface appearance

· Electrical conductivity

· Optical clarity in comparison to conventionally filled polymers

2.4 *Method of synthesis*

2.4.1 Vapor route

Under this route there are three sub divisions:

Physical vapor deposition

Chemical vapor deposition

Spray conversion processing

2.4.2 Physical vapor deposition

PVD involves the generation of vapor phase species either via evaporation, sputtering, laser ablation or ion beam. In evaporation, atoms are removed from the source by thermal or electronic means; in sputtering, atoms are ejected from the target surface by the impact of energetic ions [7]. In the former case, the vapor phase species that experience collisions and ionization are condensed onto a substrate followed by the nucleation and growth. Thermal evaporation has a limitation in multi component materials since one of the metallic elements typically evaporates before the other due to the differences in vapor pressures of the evaporating species.

On the contrary, sputtering is capable of depositing high melting point materials such as refractory metals and ceramics, which are difficult to fabricate using evaporation.

2.4.3 Chemical vapor deposition

Chemical vapor deposition (CVD) is a process where one or more gaseous adsorption species react or decompose on a hot surface to form stable solid products. The main steps that occur in the CVD process can be summarized as:

(a) Transport of reacting gaseous species to the surface.

(b) Adsorption of the species on the surface.

(c) Heterogeneous surface reaction catalyzed by the surface.

(d) Surface diffusion of the species to growth sites.

(e) Nucleation and growth of the film.

(f) Desorption of gaseous reaction products and transport of reaction products away from the surface[8,9].

2.4.4 Spray conversion processing

This route involves the atomization of chemical precursors into aerosol droplets that are dispersed throughout a gas medium. The aerosols are then transported into a heated reactor where the solution is

evaporated or combusted to form ultrafine particles or thin films [10].

2.4.5 Liquid route

Solution-based processing routes used for the synthesis of nano-particles include precipitation of solids from a supersaturated solution , homogeneous liquid phase chemical reduction and ultrasonic decomposition of chemical precursors .

2.4.6 Sol-gel process

The sol–gel processing method has been used for producing metal oxide and ceramic powders with high purity and high homogeneity for many years. The sol–gel route offers a degree of control of composition and structure at the molecular level. The process involves the generation of a colloidal suspension (‘sols’) which are subsequently converted to viscous gels and solid materials [11, 2].

2.4.7 Electro-deposition:

Electro-deposition is an electrode reactions involving oxidation/reduction of a solid metal and its dissolved ion. e.g., if a copper metal rod is immersed in a copper sulphate solution, the copper cations can be cathodically reduced to copper metal, or the copper metal can be anodically oxidized to copper ions. Compare with a redox reaction where both the oxidized and the reduced species are in solution .The terms "Electro-deposition", "Electro-dissolution" are often used to describe these reactions.

2.5 SOLID ROUTE

Mechanical Alloying and mechanochemical synthesis

Mechanical alloying

Mechanical alloying was originally invented as a method to manufacture oxide dispersion strengthened nickel alloys It is a high energy ball milling process, where alloying is the result of the repeated fracture and cold welding of the component particles. Highly meta-stable materials such as amorphous alloys and nano structured materials can be prepared by the process. Scaling up to industrial quantities seems straight forward. In addition to attrition and agglomeration, high energy milling can induce chemical reactions, which can be used to influence the milling process and the properties of the product. This fact was utilized to prepare magnetic oxide-metal nano-composites via mechanically induced displacement reactions between a metal oxide and a more reactive metal. High energy ball milling can also induce chemical changes in non-metallurgical binary systems, including silicates, minerals, ferrites, ceramics, and organic compounds. The research area of mechano-chemistry was developed to study and utilize these processes. As many mechanical alloying processes involve chemical changes, the distinction between mechanical alloying and mechano-chemistry is often arbitrary [2].

2.5.1 General description

Mechanical alloying, MA, was developed in 1960 by the International Nickel Company (INCO) as a technique for dispersing nanosized oxide inclusions into nickel-based super-alloys for gas turbine applications. The ball milling process has been successfully used and accepted as an industrial processing method because it is a simple, scaleable and inexpensive technique to prepare a variety of equilibrium and non-equilibrium alloy phases, including solid solutions, intermetalics, quasycristals, nano-structured materials, amorphous alloys and bulk metallic glasses of commercially useful and scientifically interesting materials with a number of novel properties [12].

Mechanical alloying is a process involving repeated cold welding, fracturing, and re-welding of powder particles in a high-energy ball mill. Such a process can result in the formation of an alloy with nanometer-sized grains. During the mechanical alloying process, the powder particles are periodically trapped between colliding balls and are plastically

deformed. Such a feature occurs by the generation of a large number of dislocations as well as other lattice defects. Furthermore, the ball collisions cause fracturing and cold-welding of the elementary particles, forming clean interfaces at the atomic scale .This leads to an increase of the interface number while the sizes of the components area decrease from millimeter to sub micrometer dimensions. Concurrently to this decrease of the elementary distribution, some crystalline and nano-crystalline intermediate phases are produced inside the particles involving chemical changes [13].

Grinding laws

They establish the relationship between energy required and the size range of the particles

KICK'S LAW:

$W_K=C_K\,(\ln d_A-\ln d_E)$; $d_A>50$mm

BOND'S LAW:

$W_B=C_B\,(d_E^{-1/2}-d_A^{-1/2})$; $50>d>0.05$ mm

RITTINGER'S LAW:

$W_R=C_R\,(1/d_E-1/d_A)$; $d<0.05$ mm

Where

W=energy

C=constant,

d_A=initial size,

d_E=final size

2.5.2 The most important attributes of mechanical alloying are the following [14]:

- Production of fine dispersions of second-phase particles
- Extension of solid solubility limits
- Refinement of grain sizes down to nanometer range
- Synthesis of novel crystalline and quasi-crystalline phase

- Development of amorphous (glassy) phase
- Disordering or ordered inter-metallics
- Fabrication of materials with a precise composition and controlled
- microstructure
- Possibility of alloying elements difficult to combine by conventional melting
- methods
- Inducement of chemical reactions at low temperatures
- Scalable process

2.5.3 Applications of Mechanical alloying

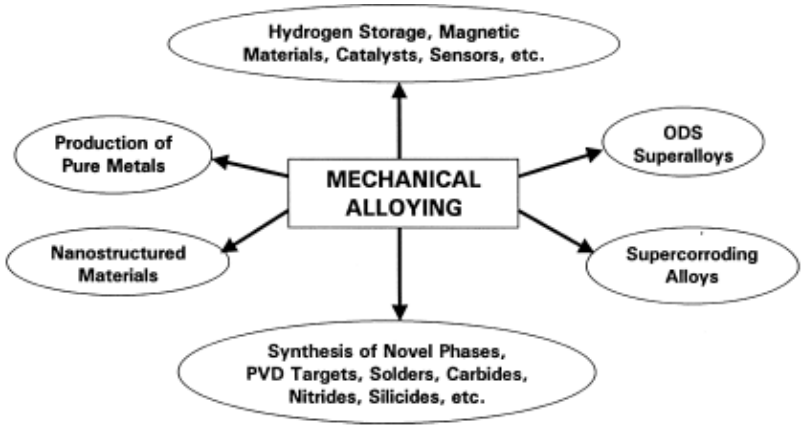

Fig 2.1 application of mechanical alloying

2.5.4 Equipment for ball milling [14]

There are different machines available for mechanical alloying. These differ in their capacity, speed of operation, efficiency of milling and additional arrangement for cooling, and heating among others.

The Spex shaker mill is used for exploratory investigations in the laboratory and screening purposes. It has one jar containing the grinding and powder sample. The jar moves describing a shape of an infinity symbol (∞) energetically several thousand times per minute.

The planetary ball mill was employed in the present research .This type of ball milling equipment is used to produce less than hundred grams of powder. Its name represents the planet-like movement of its two jars on a rotating support disk. Both jars rotate around their own axes.

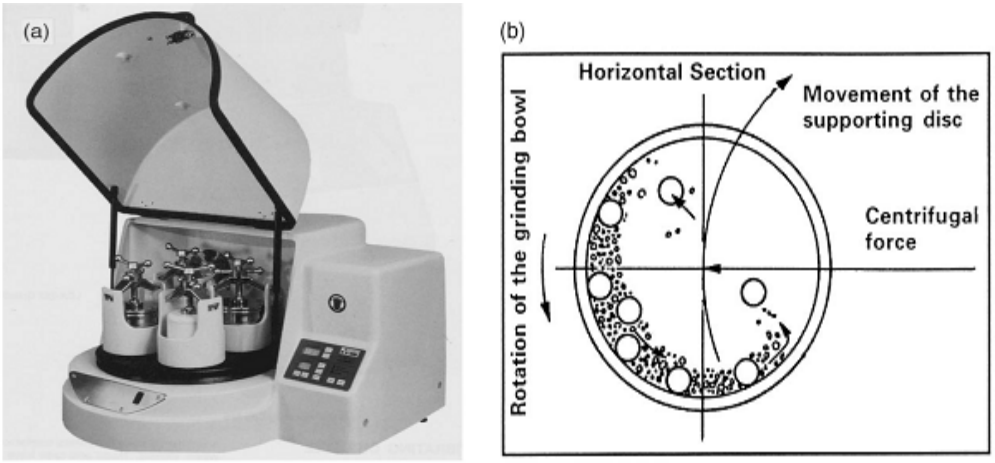

Figure 2.2: (a) Fritsch Pulverisette P4™ Vario-planetary ball milling machine with two vials mounted on supporting disk (b) working principle of the machine

The containers and the supporting disk rotate in opposite direction producing centrifugal forces that alternately act in the same and opposite directions. This causes two different effects:

Friction effect: The grinding balls run down inside jar walls

Impact effect: The sample material and balls lift off and travel freely through the inner container and collide with the opposite walls. This effect increases each time the balls crash one onto another. The impact energy depends on the speed (RPM) selected and can reach 20 times the acceleration of gravity. If the speed is reduced the impact energy is reduced and only mixing occurs.

2.5.5 Process variables in milling

To achieve the adequate product phase, microstructure, particle size and/or properties, the optimization of a number of variables involved during MA has to be considered. The following variables have an important effect in the final product after ball milling [13]:

Milling container (vial, jar, vessel, bowl)

Hardened steel, tempered steel, stainless steel, tungsten carbide, are the most common types of materials used for the grinding vessels. The material of the jar can alter the composition of the material to be mechanically milled because of the high impact and wear. The internal design of the container is important to avoid dead zones, or where the composition does not get milled; flat
ended or round ended jars are used.

Milling atmosphere

To avoid contamination and to minimize oxidation of the milled powder, MA can be conducted under vacuum or under an inert atmosphere (nitrogen/argon). The atmosphere influences the kinetics of alloying behavior of transformations and new compounds formation.

Milling speed

Milling intensity or milling energy are terms used to describe the velocity of the milling process. The faster rotation of the milling the higher input energy into the material being processed i.e. higher kinetic energy of the grinding medium imparted to the composition upon ball-milling.

Increasing the milling speed results in excessive wear of the milling tools and leads to the contamination of the material composition. Additionally, the temperature of the jar may reach a high value accelerating the transformation process by forming supersaturated solid solutions or meta-stable phases. When a critical speed occurs, the balls are pinned to the inner walls of the jar and do not fall down to exert any impact force, so the maximal speed should be below that critical value to ensure the maximal collision energy. High speed can promote higher degree of plastic deformation and cold welding so the material gets stuck to the inner walls of the container.

Grinding medium

This parameter affects directly the efficiency of the alloying. The impact force on the powder should be high enough to promote mixing and mechanical alloying, and is affected by the size, density and material of the balls. High density of the grinding medium represents high kinetic energy to be transferred to the powder. Materials commonly used are hardened steel, hardened chromium steel, stainless steel, and WC-Co. Small ball sizes (soft milling) promote intense frictional action which benefits the formation of solid solutions and amorphous phases in the final constitution. Also the attained grain size is finer with smaller balls. Large ball sizes (hard milling) result in only the mixing of components and produce high temperature which leads to the decomposition of meta-stable solid solutions.

Extent of container filling

To permit the movement and energy of impact forces exerted on balls and powder particles, enough free space in the jar is essential. About 50% of the vial space is left empty.

Ball-to-powder weight ratio (BPR)

Sometimes BPR is referred as the charge ratio, an important variable that affects the time of process. It varies from a value as low as 1:1 to one as high as100:1. Those ratios depend on special desired features, crystalline sizes, particular phase formation, micro-hardness and other final results. The higher the BPR the shorter the milling time and faster the MA. At a high BPR the mean free path decreases, and the plastic deformation increases by the increment in number of collisions per unit time; so more energy and temperature is transferred to the powder particle resulting in a faster alloying. Higher BPR can be obtained also without changing the number of balls but increasing the diameter of them or by using higher density of materials such as WC rather than steel. Lower ball to powder weight ratio results in longer times of processing to reach specific properties but increases the amount of material processed and its crystalline size.

Milling time

This is one of the most important parameters and is chosen to achieve a steady state between fracturing and cold welding of the materials in the container to facilitate the alloying. Times of process are short for high BPR values and extended for low BPR values, as explained previously

The attritor mill is used for large quantities of powders milled at a time and consists of a vertical drum containing a series of rotating impellers moved by a powerful engine. The impellers agitate the steel balls into the drum at a high velocity to impact the powder.

2.5.6 Mechanism of alloying

Different types of materials including ceramic, metallic, polymer and composites are synthesized by ball milling. A large number of phases can be formed depending on each alloy system. The mechanism through which the new alloy phases are reached is explained below:

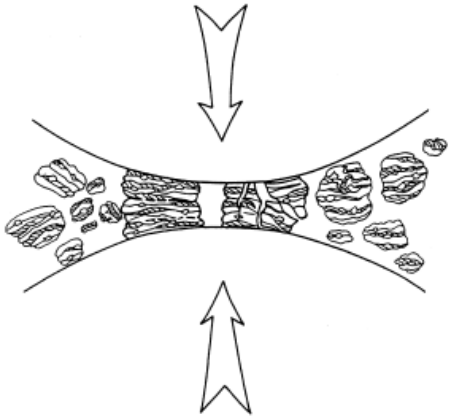

Fig 2.3: entrapment of powder particles between colliding balls

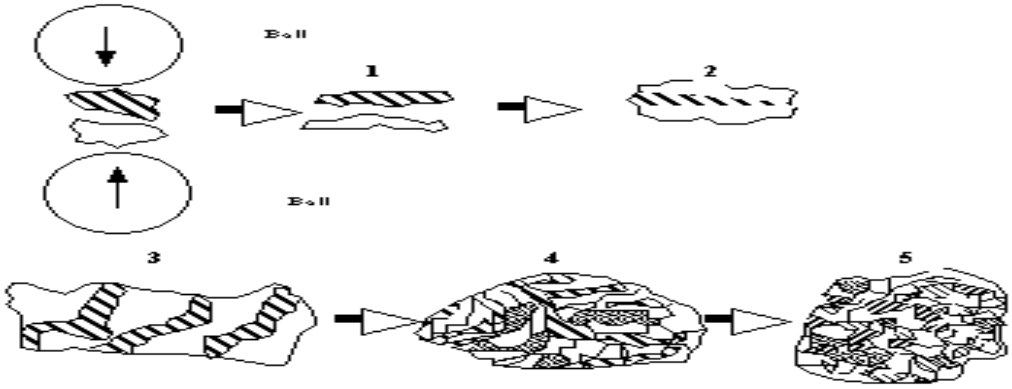

Fig 2.4: Steps in M.A process

During the collisions ball-powder-ball the powder for MA is subject to heavy deformation into the grinding medium. The powder particles are repeatedly flattened, cold welded, fractured and re-welded. For ductile materials, the effect of the collision produce material gets flattened whereas the brittle inter-metallic gets fragmented and size refined.

Every time two grinding balls smash or collide together, a small amount of powder or material is trapped between them and goes through three different stages. On average, around 1000 particles are trapped during each collision. Throughout the process of BM the powder morphology is modified in two dissimilar ways. If the starting material is ductile form layers that overlap structuring composite cold welds between them with different composition. The brittle constituents have a tendency to become occluded by the ductile component and trapped in the composite. These processes of cold welding and fracturing occur continually during the milling time leading at the end to a homogenized and refined

composition. In the early stage of the process, the chemical composition of particles varies significantly from particle to particle. The prevalence in the first stage is a lamellar structure with particle sizes that varies from few micrometers to few hundred micrometers. In the intermediate stage as the milling process continues more cold working takes place accompanied with micro-structural refinement, introduction of vacancies, dislocations, and grain boundaries. Diffusion paths are created by an increase in temperature due to the collisions between powder and ball-ball / ball-wall. Alloy formation occurs in this stage. During the final stage the lamellae microstructure becomes uniform, finer with a homogeneous composition achieving a steady state. The micro-hardness of the particles attains a high level due to the strain energy accumulated during the process [14].

2.6 CHARTERISATION TECHNIQUES

2.6.1 X-RAY DIFFRACTION

X-ray scattering techniques are a family of non-destructive analytical techniques which reveal information about the crystallographic structure, chemical composition, and physical properties of materials and thin films.

These techniques are based on observing the scattered intensity of an x-ray beam hitting a ample as a function of incident and scattered angle, polarization, and wavelength or energy [15].

The mechanical assembly that makes up the sample holder, detector arm and associated gearing is referred to as goniometer. The working principle of a Bragg-Brentano para focusing (if the sample was curved on the focusing circle we would have a focusing system) reflection goniometer is explained below. The distance from the X-ray focal spot to the sample is the same as from the sample to the detector. If we drive the sample holder and the detector in a 1:2 relationship, the reflected (diffracted) beam will stay focused on the circle of constant radius [15]. The detector moves on this circle.

The crystallite size and lattice strain in the powder particles can be determined by the X-ray peak broadening techniques. X-ray diffraction peaks are broadened due to [16]:

1. Instrumental effects,
2. Small particle size,
3. Lattice strain in the material.

However, if one is interested only in following the trend of change of crystallite size with milling conditions, this simple technique may be acceptable. While the X-ray peak broadening due to small crystallite size is inversely proportional to cosθ. The crystallite size is determined by measuring the Bragg peak width at half the maximum intensity and putting its value in scherrer's formula.

Scherrer formula:

The basis of simple size-strain analysis is the following two formulas

The Scherrer formula [16]

Crystallite size (average) = K λ / (B cos θ)

Tangent formula:

Lattice strain (mean lattice distortion) = B / (4 tan θ) [16]

B describes the structural broadening, which is the difference in integral profile width between a standard and the unknown sample:

B (size) = $B_{obs.}$ - $B_{std.}$

B (strain) = Square root ($B_{obs.}^2$ - $B_{std.}^2$)

For the calculations the broadening must be in [radians].

2.6.2 Scanning electron microscope:

The **scanning electron microscope** (**SEM**) is a type of electron microscope that images the sample surface by scanning it with a high-energy beam of electrons in a raster scan pattern. The electrons interact with the atoms that make up the sample producing signals that contain information about the sample's surface topography, composition and other properties such as electrical conductivity.

In a typical SEM, electrons are thermionically emitted from a tungsten filament cathode and are accelerated towards an anode. Tungsten is normally used in thermionic electron guns because it has the highest melting point and lowest vapor pressure of all metals, thereby allowing it to be heated for electron emission. Other electron sources include lanthanum hexaboride (LaB_6) cathodes, which can be used in a standard tungsten filament SEM if the vacuum system is upgraded. Electrons can also be emitted using a field emission gun (FEG).

The electron beam, which typically has an energy ranging from a few hundred eV to 40 keV, is focused by one or two condenser lenses into a beam with a very fine focal spot sized 0.4 nm to 5 nm. The beam passes through pairs of scanning coils or pairs of deflector plates in the electron column, typically in the final lens, which deflect the beam horizontally and vertically so that it scans in a raster fashion over a rectangular area of the sample surface.

When the primary electron beam interacts with the sample, the electrons lose energy by repeated scattering and absorption within a teardrop-shaped volume of the specimen known as the interaction volume, which extends from less than 100 nm to around 5 µm into the surface.

The size of the interaction volume depends on the electron's landing energy, the atomic number of the specimen and the specimen's density. The energy exchange between the

electron beam and the sample results in the reflection of high-energy electrons by elastic scattering, emission of secondary electrons by inelastic scattering and the emission of electromagnetic radiation which can be detected to produce an image [17].

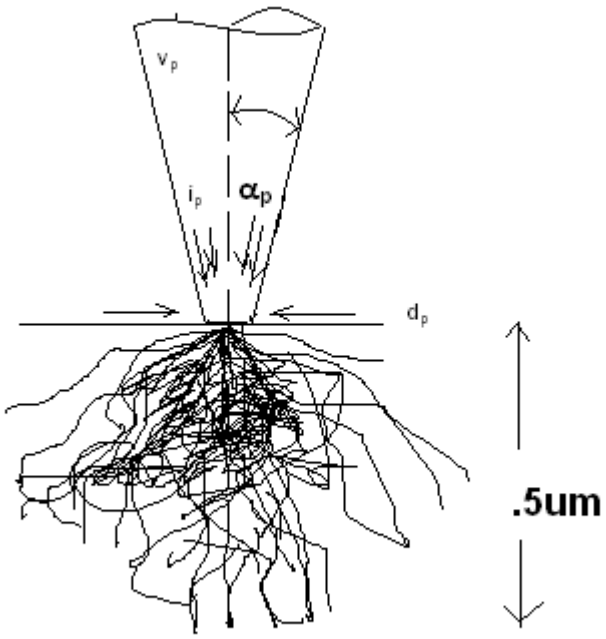

Fig 2.5: Interaction volume for a 20 Kev beam

2.6.3 Energy dispersive X-Ray analysis:

EDX Analysis stands for Energy Dispersive X-ray analysis. It is sometimes referred to also as EDS or EDAX analysis. It is a technique used for identifying the elemental composition of the specimen, or an area of interest thereof.

The EDX analysis system works as an integrated feature of a scanning electron microscope (SEM), and can not operate on its own without the latter.

During EDX Analysis, the specimen is bombarded with an electron beam inside the scanning electron microscope. The bombarding electrons collide with the specimen atoms' own electrons, knocking some of them off in the process. A position vacated by an ejected inner shell electron is eventually occupied by a higher-energy electron from an outer shell. To be able to do so, however, the transferring outer electron must give up some of its energy by emitting an X-ray.

The amount of energy released by the transferring electron depends on which shell it is transferring from, as well as which shell it is transferring to. Furthermore, the atom of every element releases X-rays with unique amounts of energy during the transferring process. Thus, by measuring the amounts of energy present in the X-rays being released by a specimen during electron beam bombardment, the identity of the atom from which the X-ray was emitted can be established.

The output of an EDX analysis is an EDX spectrum. The EDX spectrum is just a plot of how frequently an X-ray is received for each energy level. An EDX spectrum normally displays peaks corresponding to the energy levels for which the most X-rays had been received. Each of these peaks is unique to an atom, and therefore corresponds to a single element. The higher a peak in a spectrum, the more concentrated the element is in the specimen [17].

An EDX spectrum plot not only identifies the element corresponding to each of its peaks, but the type of X-ray to which it corresponds as well. For example, a peak corresponding to the amount of energy possessed by X-rays emitted by an electron in the L-shell going down to the K-shell is identified as a K-Alpha peak. The peak corresponding to X-rays emitted by M-shell electrons going to the K-shell is identified as a K-Beta peak. See Figure.

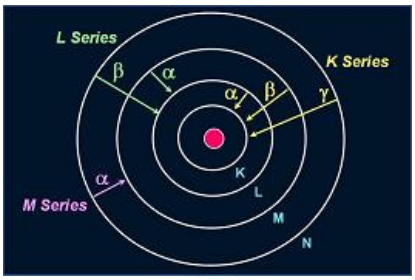

Fig 2.6: Elements in an EDX spectrum are identified based on the energy content of the X-rays emitted by their electrons as these electrons transfer from a higher-energy shell to a lower-energy one.

2.6.4 Fourier transforms infra red spectroscopy (FTIR):

FTIR (Fourier Transform Infrared) Spectroscopy, or simply FTIR Analysis, is a failure analysis technique that provides information about the chemical bonding or molecular structure of materials, whether organic or inorganic. It is used in failure analysis to identify unknown materials present in a specimen, and is usually conducted to complement EDX analysis.

The technique works on the fact that bonds and groups of bonds vibrate at characteristic frequencies. A molecule that is exposed to infrared rays absorbs infrared energy at frequencies which are characteristic to that molecule. During FTIR analysis, a spot on the specimen is subjected to a modulated IR beam. The specimen's transmittance and reflectance of the infrared rays at different frequencies is translated into an IR absorption plot consisting of reverse peaks. The resulting FTIR spectral pattern is then analyzed and matched with known signatures of identified materials in the FTIR library.

Unlike SEM inspection or EDX analysis, FTIR spectroscopy does not require a vacuum, since neither oxygen nor nitrogen absorbs infrared rays. FTIR analysis can be applied to minute quantities of materials, whether solid, liquid, or gaseous. When the library of FTIR spectral patterns does not provide an acceptable match, individual peaks in the FTIR plot may be used to yield partial information about the specimen.

Single fibers or particles are sufficient enough for material identification through FTIR analysis. Organic contaminants in solvents may also be analyzed by first separating the mixture into its components by gas chromatography, and then analyzing each component by FTIR.

Molecules and crystals can be thought of as systems of balls (atoms or ions) connected by springs (chemical bonds). These systems can be set into vibration, and vibrate with frequencies determined by the mass of the balls (atomic weight) and by the stiffness of the springs (bond strengths). The mechanical molecular and crystal vibrations are at very high frequencies ranging from 10l2 to 1Ol4Hz (3-300 km wavelength), which is in the infrared (IR) regions of the electromagnetic spectrum.

In the infrared experiment, the intensity of a beam of infrared radiation is measured before and after it interacts with the sample as a function of light frequency. **A** plot of relative intensity versus frequency is the "infrared spectrum." **A** familiar term "FTIR' refers to Fourier Transform Infrared Spectroscopy, when the intensity-time output of the interferometer is subjected to a Fourier transform to convert it to the familiar infrared spectrum (intensity-frequency) [18, 19].

Interactions of electron beam with sample*:*

I) When a beam of parallel monochromatic radiation enters an absorbing medium at right angles to the plane parallel to the surface of the medium then each infinitesimally small layer of the medium decreases the intensity of the beam by a constant fraction.

II) When a monochromatic light passes through a transparent medium rate of decrease in intensity with the thickness of the medium is proportional to intensity of light

III) Intensity of a beam of monochromatic light decreases exponentially as the concentration of the absorbing substance increases arithmetically

Log (T)= - abc

Where,

T-Transmittance

a-absorbance

b-optical path

c-concentration

2.6.5 Sintering behaviour and mechanical properties of nanostructured materials:

Sintering is essentially a process of incipient fusion in which a material is just heated up to the brink of its melting point. The densification process of solid particle bonding or neck formation is usually followed by continuous elimination of pores to enable production a pore free body. Solid state densification in general can be divided into three stages: initial, intermediate and final. Multiple mechanisms may incur during the course viz. evaporation-condensation, surface diffusion, grain boundary diffusion, bulk diffusion, viscous flow, and plastic deformation.

In conditions of neck formation surface diffusion may be accepted as the dominating mechanism during initial stages. Surface diffusion is expected to be extremely rapid in early sintering stages for nanoparticles having high surface areas.

Surface diffusion does not lead to densification due to grain coarsening in case of conventional powders. Better surface diffusion in accordance with reduced low –temperature densification should be observed in sintering nanoparticles. This is a corollary, since for nanoparticles, enhanced low temperature diffusion has been observed. Molecular dynamics also indicate extremely fast sintering behavior of nanoparticles. Even surface diffusion cannot correlate the corresponding anomaly in this behavior. Usage of higher rates of heating to avoid deleterious surface diffusion doesn't seem beneficial for small powders whereas, seldom small heating rates induce high densities. Notice of effect of heating rates has not been observed on densification or grain growth. A major contribution of surface diffusion upon overall densification is not known and it may differ when compared to conventional materials .In comparison to conventional sintering grain boundary diffusion is evident in nanopowders.

Mechanisms responsible for neck formation in nanopowders are as viz. grain boundary slip, dislocation motion, grain rotation, viscous flow and even grain boundary melting.

Materials offering obstruction to mobility of dislocations, such as intermetallic compounds viscous flow is predominant towards neck formation and growth. Further densification can be achieved though grain boundary sliding.

Greater magnitude of grain boundary stresses may cause melting or amorphization which in turn enhances densification.

Normally sintering cannot be achieved through multiple mechanisms. Specific mechanisms cannot be identified since they vary during course of sintering. As a consequence interpretation of Arrhenius plots becomes quite cumbersome. In addition to this domination of sintering mechanisms change with particle size. In addition to this domination of sintering mechanisms change with particle size. The greatest ambiguity has been observed during initial stages of sintering. For later sintering stages activation energies match with values determined during sintering of conventional powders.

Sintering is critically dependent upon particle surface condition. Particle surface properties affect mechanical properties in addition to individual particle properties and sintering behavior too. So precautions should be taken to avoid in-situ consolidation of nanopowders.

MECHANICAL PROPERTIES:

Conventional polycrystalline materials show an increase in yield strength with decrease in grain size which can be explained by the Hall-Petch equation:

$\sigma_y=\sigma_0+kd^{-1/2}$

Where σ_y=yield strength

σ_0=yield strength at infinite grain diameter

k =locking parameter (Hall-Petch slope)

In analogy, hardness (Hv) can be related to the grain size by

$Hv = H_0 + k_H d^{-1/2}$

where H0 and kH are constants. Hardness is a measure of the resistance of a material to plastic deformation under the application of indenting load. The Hall–Petch effect in conventional coarse-grained materials is attributed to the grain boundaries acting as obstacles to dislocations nucleated mostly from Frank–Read sources. Consequently, a dislocation pileup can be formed against a grain boundary inside a grain

By decreasing the grain size of metals down to the order of a few tens of nanometers, the Hall–Petch slope remains positive but with a smaller value. At ultra-fine grained sizes below 20 nm, a reversed softening effect or negative Hall–Petch relation is observed for some metals. Grain boundary sliding, creep diffusion, triple junctions, pores and impurities could contribute to inverse Hall–Petch relation in metals and alloys.

CHAPTER 3

EXPERIMENTAL SECTION

Powder blends of elemental (>99.5 wt % purity) Al, Mn and Ce (<70 μm particle size) having nominal compositions of $Al_{90}Mn_8Ce_2$ (in at. %) were ball milled in a high energy Fritsch Pulverisette-5 planetary mill in cemented carbide grinding media at a mill speed of 300 *r.p.m.* and a ball to powder ratio 10:1, using toluene as the process control agent. The identity and phase evolution at different stages of MA were studied by the X-ray diffraction (XRD) analysis of the milled powders using the Cu-Kα radiation (λ = 1.540598 nm) in a Philip's X'pert Pro high-resolution x-ray diffractometer. Crystallite size and lattice strains for different milling h were calculated using the Scherrer formula. SEM and EDS studies of the powders were carried out in a Jeol JSM LV 7680 scanning electron microscope. FTIR study of the powders milled for different h was also carried out.

Final powder of milled for 86 h was compacted at 10-12 ton loads. These specimens were measured for green density and subsequently sintered in nitrogen and hydrogen atmospheres at different temperatures. After sintering, sintered compacts were again analyzed for density and X-ray diffraction.

Mechanical properties especially, hardness of green and sintered compacts was measured by Leco LV 700 micro hardness tester and compared with sintering conditions.

CHAPTER 4

Results and Discussion

4.1 X-Ray diffraction results

XRD results confirm that at o h the powder material contains only Al,Mn&Ce while as the milling h increase formation intermetallic compounds take place.For higher milling h the peaks are not distinctly visible due to broadening.So we have divided the plot into two regions viz. low angle region & high angle region which also confirm that peak broadening has taken place.The reasons behind broadening has been mentioned in chapter 2.

Phase Analysis of powder material:

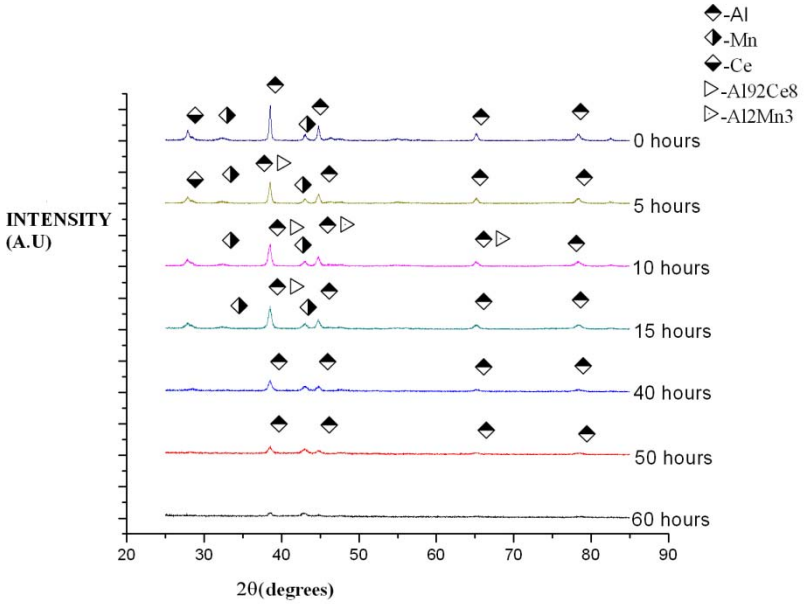

Fig 4.1.1 XRD spectra of the milled samples

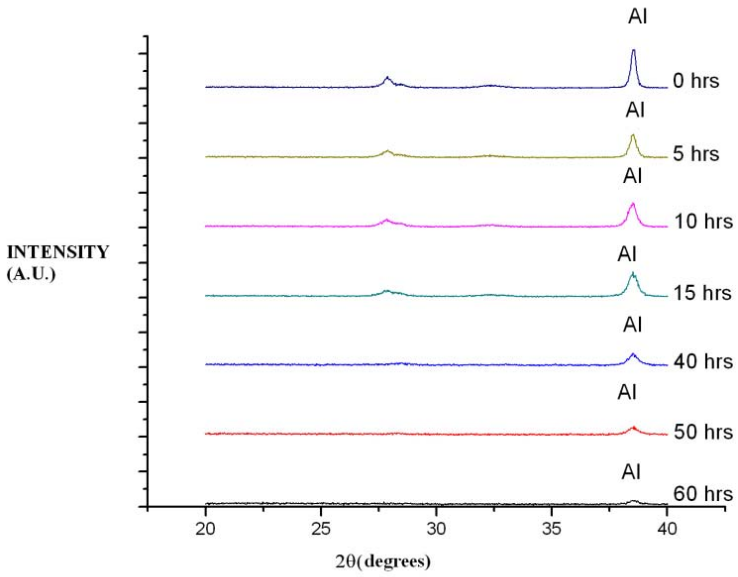

Fig 4.1.2 Low angle region showing broadening of Al peak

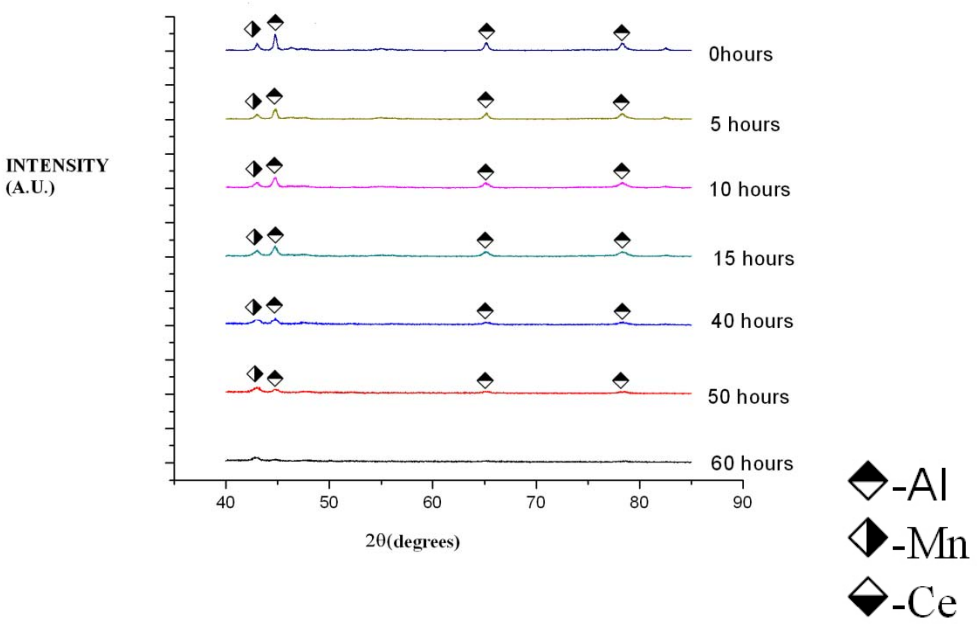

Fig 4.1.3 High angle region

With increase in milling h or decrease in size ,we observe that there is a decrease in the intensities of the peaks. The comparison of the diffractograms reveals progressing line broadening as a function of time of milling. As the milling h increase the other constituents are not detected as they are incorporated into the matrix. Intermetallic compounds, possibly $Al_{92}Ce_8$ and Al_2Mn_3 are formed.

Phase analysis of Sintered compacts in N_2 and H_2 atmosphere at different temperatures

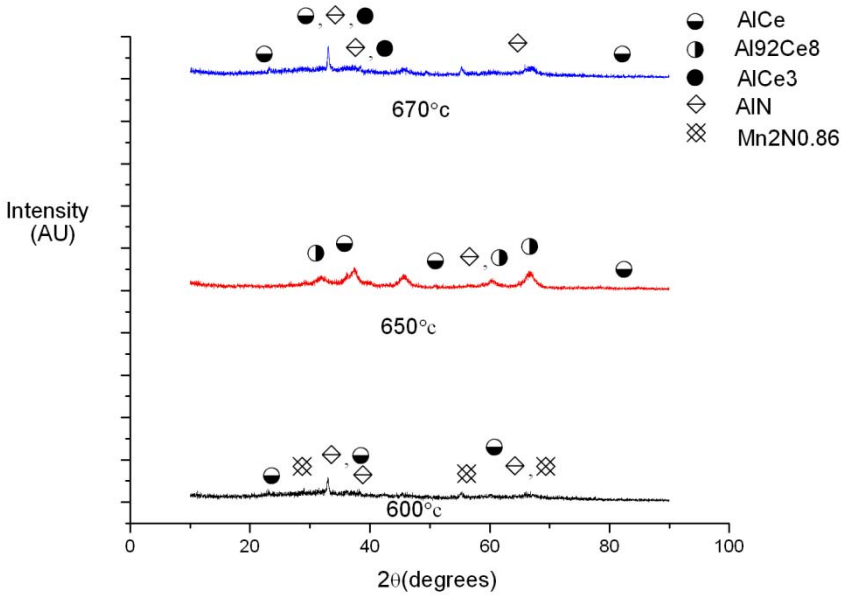

Fig 4.1.4:Phase analysis of specimens sintered in N_2 atmosphere at different temperatures

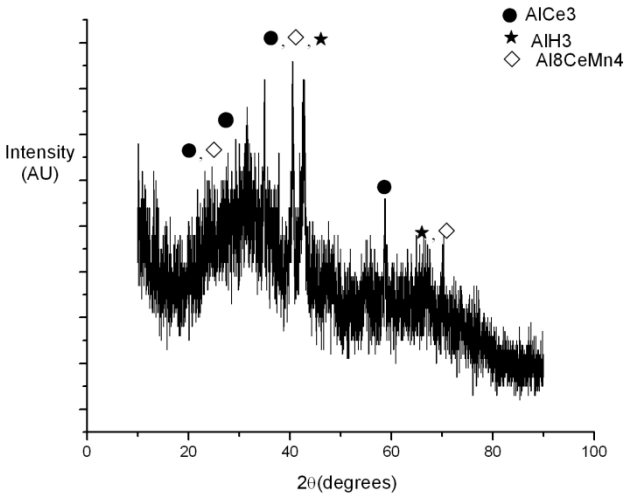

Fig 4.1.5: Phase analysis of sintered compacts in hydrogen atmosphere at 600°C

Calculation of Crystallite size and lattice strain:

Table 1: Calculated grain size and lattice strain results from the samples with different milling time.

Serial no	Milling time(h)	Crystallite size(nm)	Lattice strain (%)
1	5	105.2	.252
2	10	59.3	.369
3	15	43.4	.449
4	40	36.6	.502
5	50	35.5	.512
6	60	33.4	.523

The given values are calculated according to the Scherrer formula as given in chapter 3. It can be observed that grain/crystallite size has got reduced as the milling time progresses at first and then gradually evens out due to work hardening. The observed value are represented graphically in fig 4.1.6

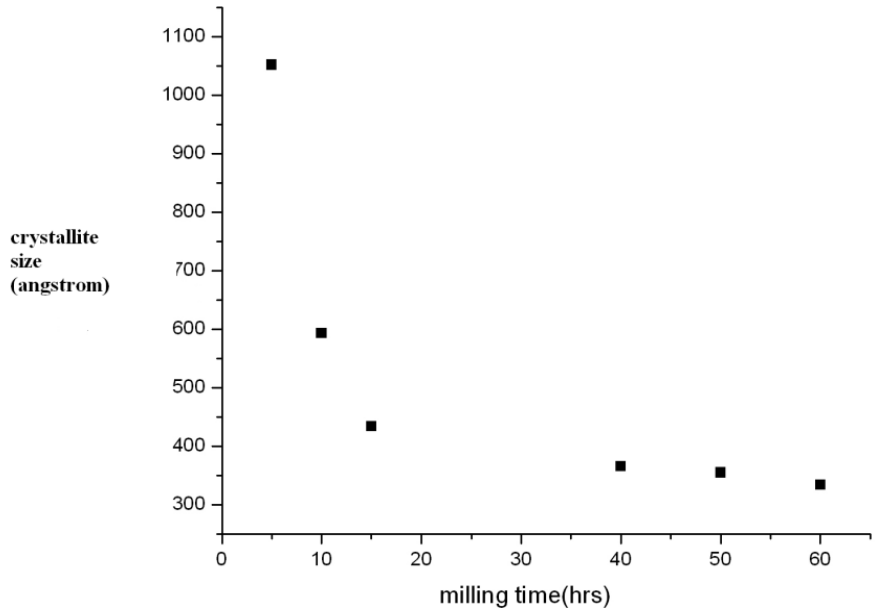

Fig 4.1.6: Milling Time versus crystallite size (of Al) plot:

4.2 SEM & EDS RESULTS

Figure shows magnified images of the samples milled at the respective h as depicted in the figure. It can be observed that the white phase is gradually vanishing where as the gray phase is getting richer in appearance.

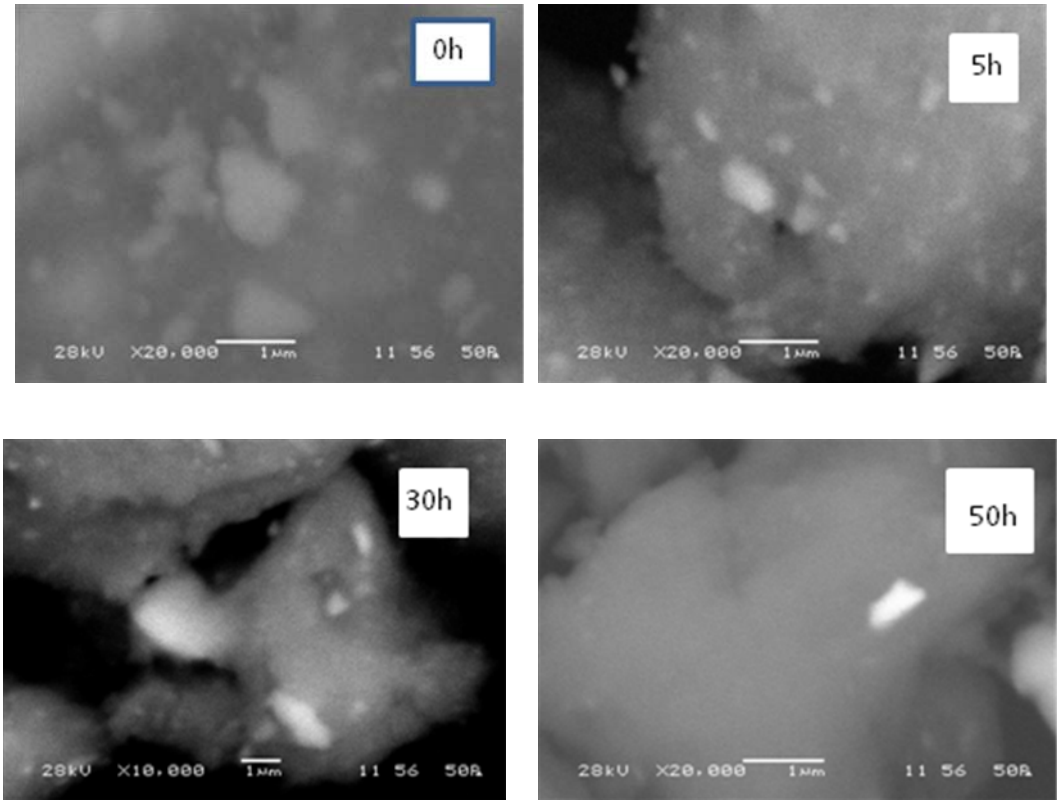

Fig 4.2.1: SEM micrographs for different powder samples milled for different h

A more critical analysis has been given in fig. for 0 hour and 5 h with their corresponding EDS analysis. The result shows that the bright phase is rich in aluminium and the dark phase contains less of aluminium. The complete elemental analysis of the nanocomposite along with the oxidation tendency is given in table2. With increase of milling h oxygen content is getting increased. The above result supports the fact that decreased grain size favors greater extent of ionic and reactivity character.

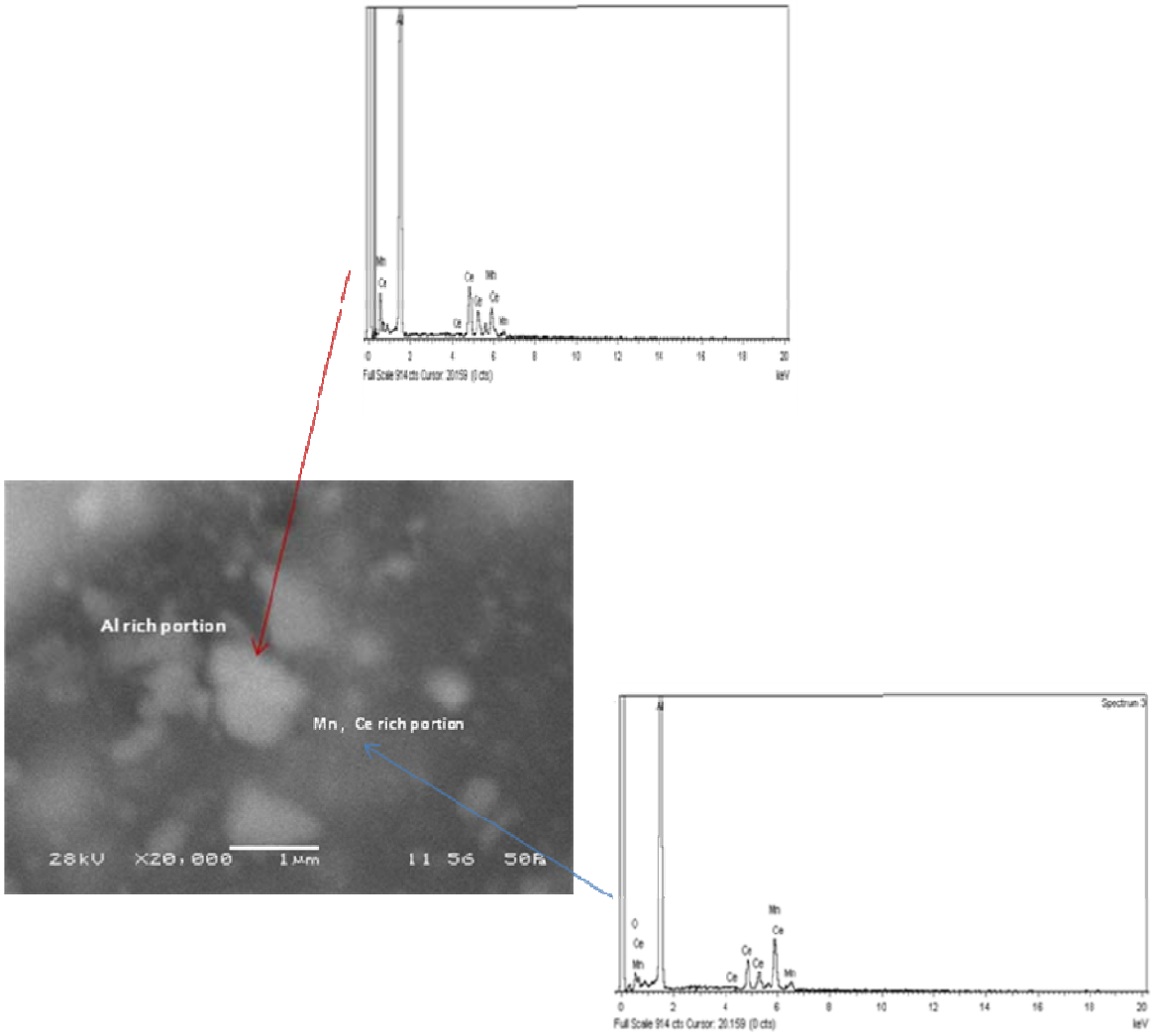

Fig 4.2.2 SEM micrograph & EDS analysis of 0 hour sample.

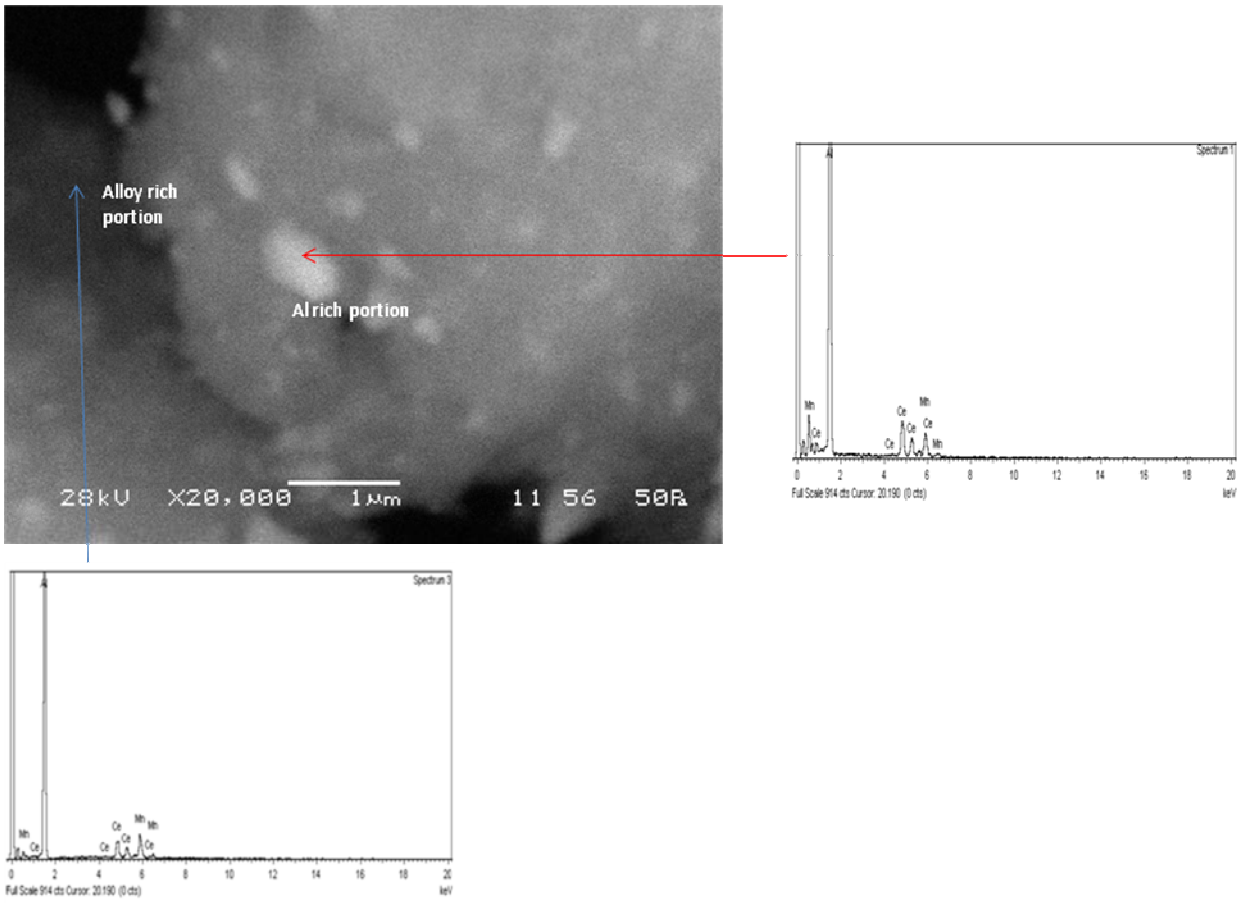

Fig 4.2.3: SEM micrograph & EDS analysis of 5 hour sample

Table 2: Elemental analysis of bright and dark phases

S.N.	Milling h		CI	CI(wo)	White phase	White phase(wo)	Grey phase	Grey phase(wo)	Dark phase	Dark phase(wo)
1	0	% Al	36.62	72.67			45.71	78.36	45.25	77.32
		% Mn	5.13	6.14			3.72	7.13	5.48	10.49
		% Ce	5.45	21.19			7.54	14.52	6.34	12.11
		%C	4.86				_	_	_	_
		% O	47.94				43.03	_	42.93	_
2	5	% Al	54.39	80.22	46.47	77.57	33.84	82.78	26.29	76.17
		% Mn	4.89	7.2	3.38	5.65	1.61	4.78	2.69	8.75
		% Ce	8.46	12.55	9.96	16.78	4.16	12.44	4.6	15.09
		%C	10.19	_	21.27	_	7.94	_	11.32	_
		% O	22.08	_	18.92	_	52.44	_	55.11	_
3	15	% Al	16.01	47.02			30.34	80.29	24.14	75.97
		% Mn	18.18	48.71			1.88	5.85	2.39	8.45
		% Ce	1.59	4.27			4.41	13.86	4.38	15.58
		%C	12.12	_			9.57	_	12.6	_
		% O	52.1	_			53.79	_	56.49	_
4	30	% Al	17.37	76.44	17.28	58.33	21.24	80		
		% Mn	2.4	12.37	1.56	6.07	1.41	6.34		
		% Ce	2.14	11.19	2.57	10.41	2.99	13.66		
		%C	16.8	_	14.61	_	14.89	_		
		% O	61.28	_	57.01	_	59.48	_		
		%w			6.96	25.19				
5	50	% Al	8.09	89.28	7.43	11.95	6.89	16	4.7	12.16
		% Mn	0.65	10.72	0.67	1.36		_		_
		% Ce				_		_		_
		%C	44.34		37.62	70.93	23.74	84	24.87	87.84
		% O	46.91		46.24	_	69.37	_	70.43	_
		%Ti			8.04	15.76				

4.3. FTIR RESULTS

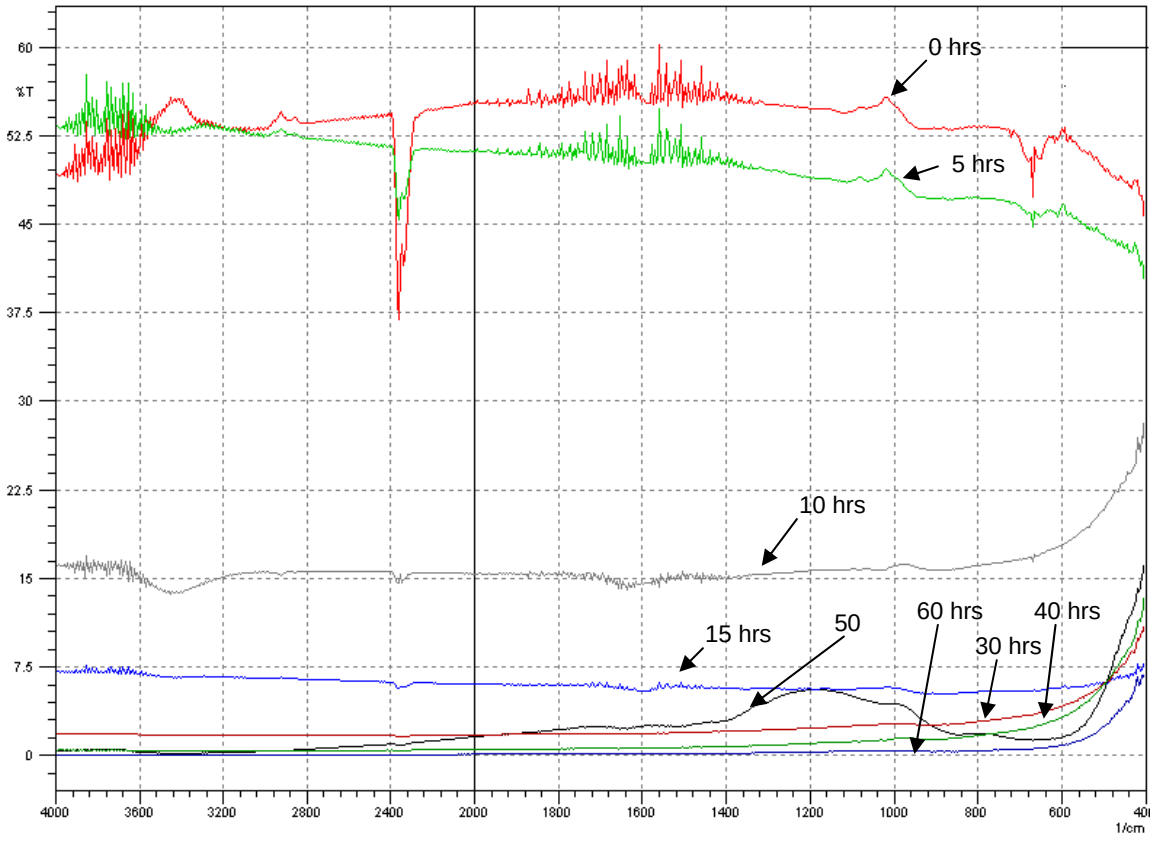

Fig 4.2.4 FTIR plot of the milled samples

As the milling h are progressing the % transmittance is getting decreased and the % absorbance is getting increased which indicates that surface integrity of the sample is improving as the milling h progress.

Plot of % transmittance v/s crystallite size:

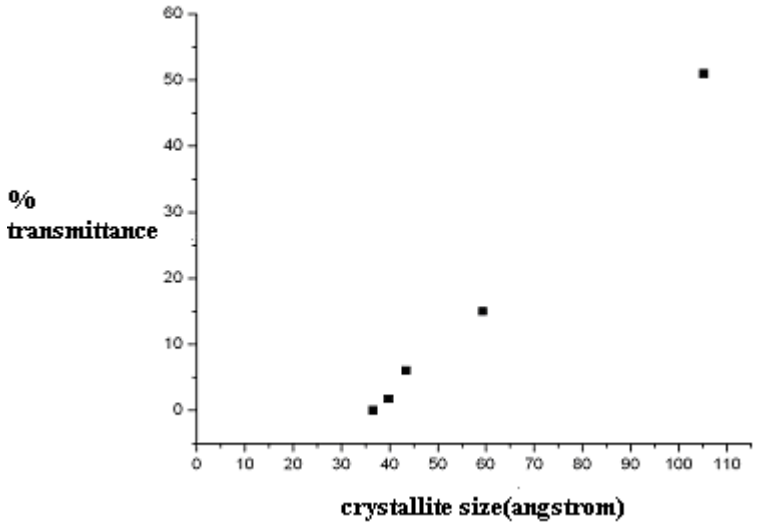

Fig 4.2.5: %transmittance vs. crystallite size plot

A decreasing trend can be observed in the above graph.

4.4 Mechanical properties of Al-Mn-Ce nanostructured material

Powdered material was compacted at loads varying between 12-15 tonnes.

Table 3 shows the density of green compacts used for sintering in N_2 and H_2 atmospheres at 600°C.

S.N.	Mass(g)	Thickness(mm)	Density(g/cc)	% densification
1	0.78	2.4	1.84	68.4
2	0.80	2.43	1.86	68.9
3	0.81	2.48	1.85	68.5
4	0.83	2.50	1.88	69.6
5	0.84	2.55	1.86	68.9
6	0.82	2.58	1.80	66.6

Average density of the green compacts =1.84 g/cc

The hardness of the sintered compacts was measured in a Leco LV 700 Microhardness tester. Average green density=29.3VHN

.

Table 4: Hardness values of sinters at different temperatures and atmospheres used for sintering in N_2 atmosphere at 600,650 and 675˚C and H_2 atmospheres at 600°C.

S.N.	Atmosphere	Temperature(°C)	Hardness (VHN)
1	N_2	600	147.23
2	N_2	650	50.7
3	N_2	675	51
4	H_2	600	148.1

We observe that specimens sintered at 600°C in N_2 and H_2 atmospheres have high hardness values of 147VHN and 148VHn respectively. This can be attributed to the high green density values of around 68% which after sintering attained a value of around 75%.Another reason for the high hardness is the presence of hard AlN and AlH_3 phases. Specimens sintered at 650 and 675°C, although expected to exhibit higher hardness values have been found to have much lower hardness values of 50 and 51VHN respectively. This anomaly can be attributed to the lower green density (approx. 57%) of the specimens which after sintering attained a density of around 65% only.

CHAPTER 5

Conclusions

1. XRD showed a compound formation between Al, Mn and Ce.
2. XRD calculations based on Scherrer formula indicated decreasing crystallite size and increasing lattice strain with increasing milling h.
3. SEM and EDX analysis showed distinct Al rich and alloy rich region.
4. FTIR results indicated increasing % absorbance and decreasing % transmittance as crystallite size decreases with increasing milling time.
5. Sintered compacts with lower density (~63%) showed very low hardness although sintering temperatures were higher (650 and 675°C), because of low green density (~57%). Compacts with higher green densities resulted in high hardness values although sintering temperatures were maintained at 600°C.
6. Sintering under N_2 and H_2 atmospheres showed the formation of nitrides and hydrides respectively. The higher hardness resulted under these atmospheres was possibly due to the formation of the above said phases as well as due to high density of the compacts.

REFERENCES

1. H. Gleiter, Prog. Mater. Sci. 33 (1989) 223.
2. S.C. Tjong, Haydn Chen Materials Science and Engineering R 45 (2004) 1–88
3. B. Harris Engineering composite materials. Second Edition; IOM communications editors. 1999, p.20-7.
4. WWW.Wikipidea.org (last updated 03/04/08)
5. www.acgroupinc.com (last updated 15/04/08)
6. Y.K. Huang, A.A. Menovsky, F.R. de Boer, Nanostruct. Mater. 2 (1993) 505.
7. S. Okuda, M. Kobiyama, T. Inami, S. Takamura, Scr. Metall. 44 (2001) 2009
8. M.L. Hitchman, K.F. Jensen, Chemical Vapor Deposition—Principles and Applications, Academic Press, London,1993
9. A. Sherman, Chemical Vapor Deposition For Microelectronics—Principles, Technology and Applications, Noyes Publications, New Jersey, 1987.
10. G.L. Messing, S.C. Zhang, G.V. Jayanthi, J. Am. Ceram. Soc. 76 (1993) 2707.
11. M. Ebelman, Ann. Chim. Phys. 16 (1846) 129.
12. Suryanarayana C. Mechanical Alloying and Milling. Marcel Dekker, New York; 2004, p.15-30
13. Dunlap R, Small D, MacKay G. Materials preparation by ball milling. Journal of physics; 2000; 78: p.211-229.
14. L. Reyes-Russi, Master Thesis, UPRM-RUM 2007
15. XRD basics,www.scintag.com(last updated 20/04/08)
16. Principles of x-ray diffraction, B.D. Cullity
17. Scanning electron microscopy and x-ray microanalysis, Joseph I. Goldstein et al

18. Yibing Cai, Qufu Wei, Fenglin Huang, Weidong Gao Preparation and properties studies of halogen-free flame retardant form-stable phase change materials based on paraffin/high density polyethylene composites Applied Energy, Volume 85, Issue 8, August 2008, Pages 765-775

19. K. Chu, Y.G. Shen Mechanical and tribological properties of nanostructured TiN/TiBN multilayer films Wear, Volume 265, Issues 3-4, 31 July 2008, Pages 516-524